Effective ice particle densities for cold anvil cirrus

Andrew J. Heymsfield, Carl G. Schmitt, and Aaron Bansemer
National Center for Atmospheric Research, Boulder, Colorado, USA

Darrel Baumgardner
Universidad Nacional Autonoma de Mexico, Mexico City, Mexico

Elliot M. Weinstock, Jessica T. Smith, and David Sayres
Harvard University, Cambridge, Massachusetts, USA

Received 1 August 2003; revised 13 October 2003; accepted 13 November 2003; published 16 January 2004.

[1] This study derives effective ice particle densities (ρ_e) from data collected by the NASA WB-57F aircraft near the tops of Florida anvils during the Cirrus Regional Study of Tropical Anvils and Cirrus Layers (CRYSTAL) Florida Area Cirrus Experiment (FACE). The ρ_e-ice particle mass divided by the volume of an equivalent diameter liquid sphere-, is obtained for particle populations ($\overline{\rho_e}$) and single sizes from a few to 200–300 μm in maximum dimension using measurements of condensed water content and particle size distributions. Density values are needed for numerical modeling of ice cloud microphysical properties and remote sensing retrievals, and have not up to now been characterized for cold ice clouds containing mixed particle habits. The $\overline{\rho_e}$ decrease with increasing slopes of gamma size distributions fitted to the size distributions, ranging from 0.15–0.91 g cm^{-3}. For single sizes, ρ_e obeys a power-law with an exponent of about −0.4. *INDEX TERMS:* 0305 Atmospheric Composition and Structure: Aerosols and particles (0345, 4801); 0325 Atmospheric Composition and Structure: Evolution of the atmosphere; 0360 Atmospheric Composition and Structure: Transmission and scattering of radiation. **Citation:** Heymsfield, A. J., C. G. Schmitt, A. Bansemer, D. Baumgardner, E. M. Weinstock, J. T. Smith, and D. Sayres (2004), Effective ice particle densities for cold anvil cirrus, *Geophys. Res. Lett.*, *31,* L02101, doi:10.1029/2003GL018311.

1. Introduction

[2] Better characterizations of ice cloud particle properties are needed to improve the representation of ice and radiation processes in mesoscale and climate models and to facilitate accurate retrievals of ice cloud properties from ground- and satellite-based remote sensors. This study focuses on a major underlying property of ice cloud particles, their masses (m) or a related property, their effective ice densities (ρ_e). Through knowledge of the density and from measurements or representations of ice particle size distributions (PSD), many ice cloud bulk properties such as the ice water content (*IWC*), the ice-mass flux (precipitation rate), and the equivalent radar reflectivity, can be derived. Without this knowledge, uncertainties in the estimates of each of these parameters may be large. There is an impending need for accurate estimates of the effective density, as algorithms for retrieving *IWC* from forthcoming satellite-based cloud radars including CloudSat will place considerable reliance on accurate estimates of ice particle density.

[3] Three methods have been used in earlier studies to estimate m or ρ_e for individual ice particles or as a function of the particle maximum dimension (D). One method (1), comprising most earlier studies, involves collecting ice particles in oil to obtain their maximum dimension, then melting them to obtain their melted equivalent diameter and mass [*Magono and Nakamura*, 1965; *Heymsfield*, 1972; *Locatelli and Hobbs*, 1974]. These relationships have almost exclusively been derived for single particle habits (e.g., hexagonal plates), or single particle types (e.g., aggregates, graupel). Method (2) uses measured *IWC* and measured PSD from airborne probes to evaluate or infer appropriate $m(D)$ relationships [*Brown and Francis*, 1995]. In method (3) if an ice crystal is one of the regular types of geometrical shapes or habits observed under certain situations in ice clouds, the projected cross-sectional particle area and an assumed bulk ice density (that accounts for hollows within crystals) is used to provide an indication of its effective density [*Heymsfield et al.*, 2002]. Analytic relationships between particle dimension and mass can then be derived.

[4] This paper extends the method of estimating ice particle mass or density for single particles or sizes and habits to the broader, more realistic case, of deriving mean effective densities for ice particle ensembles containing single or mixed particle habits. We also derive $m(D)$ relationships. The methods and the data sets are described in section 2. Results are presented in section 3. The results are summarized and conclusions drawn in section 4.

2. Methods and Measurements

[5] This section describes the methods and data sets used in this study. A detailed examination of the error sources, including possible measurement errors and biases in the estimates of ρ_e, are also discussed.

2.1. Methods

[6] The method used to calculate the average density for a population of ice particles observed per unit volume of ice cloud, $\overline{\rho_e}$, is quite simple in principal. Direct measurement of the *IWC* yields the number of grams of ice per cubic meter of air. The coincident PSD as measured by airborne particle size spectrometer are used to derive a total spherical

0094-8276/04/2003GL018311$05.00

particle volume per unit volume of air (V). This involves assuming that the measured particle population are spheres, from which

$$V = \pi/6 \Sigma N_i D_i^3, \quad (1)$$

where N_i is the ice particle concentration per size bin i and D_i is the midpoint diameter of the size bin. The $\overline{\rho_e}$ is just IWC/V. This result can readily be shown to be correct from analytic considerations by assuming exponential or gamma-type PSD [*Heymsfield et al.*, 2004], but is not shown here for brevity.

[7] The $\overline{\rho_e}$ values can be related to other properties of the PSD. The variable that is most directly related to $\overline{\rho_e}$ is the slope (tail) of the particle size distribution, λ, which can be found by fitting the N_i versus D_i measurements from the size spectrometers to a single gamma-type size distribution of the form

$$N(D) = N_0 D^{\mu} e^{-\lambda D}, \quad (2)$$

where $N(D)$ represents the concentration per unit volume per unit size, N_0 is the intercept parameter, and μ the dispersion. The moment matching method described in *Heymsfield et al.* [2002] and in references cited in that article can be used to find the coefficients for the gamma fits. The median mass diameter, D_m, can then be found analytically for a gamma distribution [*Mitchell*, 1991] from

$$D_m = (\varphi + 0.67 + \mu)/\lambda, \quad (3)$$

where φ is the exponent in the mass versus diameter power-law relationship and has a value of between about 1.7 and 2.5.

2.2. Measurements

[8] This study uses measurements obtained by the NASA WB-57F aircraft during CRYSTAL FACE in southern Florida in July 2002. The WB-57F sampled cirrus formed by two different processes: deep convection, and in-situ generation. This paper focuses on the anvils and related ice cloud produced in association with the deep convection.

[9] Particle size distributions were measured with the Droplet Measurement Technologies (DMT) Cloud, Aerosol, and Precipitation Spectrometer (CAPS) probe and a Particle Measuring Systems (PMS)/DMT Forward Scattering Spectrometer Probe (SPP-100). The Cloud and Aerosol Spectrometer (CAS) probe portion of the CAPS produces data in 20 unequally sized diameter bins between about 0.3 and 44 μm. The SPP-100 measures particles from about 3 to 55 μm. The Cloud Imaging Probe (CIP) portion of the CAPS measures from 50 to 1600 μm, with a size resolution of 25 μm. The measurements from the CAPS and the SPP-100 were combined to provide a continuous size distribution from 0.3–1600 μm [*Baumgardner et al.*, 2004]. The analysis of the current study limits the smallest size to 5 μm to minimize the possibility of including aerosols. Nonetheless, the CAS concentrations in each bin may be subject to overestimates due to the breakup of large ice particles on the inlet of the probe, an area of future study. We do not believe that the breakup issue is significant here because as noted in Section 3, we are focusing on periods where the particles are generally small. Particle sizes may also be overestimated by the assumption that the CAS particles are spheres.

[10] *Baumgardner et al.* [2004] discusses the processing algorithms for the CAS portion of the CAPS. The data were processed in 10-sec intervals to obtain a statistically accurate sample. The techniques we used to process the CIP data are given in *Heymsfield et al.* [2002]. The CIP data processing includes the technique used to reconstruct partially imaged particles by *Heymsfield and Parrish* [1978]. For each CIP interval, concentrations were derived in 19, non-equally spaced, size bins for each five seconds, or approximately 900 m of flight. The CAS and CIP data sets were merged to provide a single size distribution between 5 and 1600 μm for each 5-seconds of flight.

[11] The Harvard Total Water Instrument (TWI) [*Weinstock et al.*, 2003] samples vapor and, if present, condensate through a 1 cm (inside diameter) isokinetic inlet. A heater evaporates the condensate within the transit time from the heater to a water vapor detector, about 160 milliseconds. The total water vapor content of the ambient air is measured and the IWC is the difference in water content between the TWI and that measured by a water vapor instrument [*Weinstock et al.*, 1994] that uses the same detection technique but does not evaporate the condensate. Quoted accuracy for total water measurements range from ±5% in clear air to ±15% in clouds. Calculations suggest that solid ice spheres with diameters larger than about 50–200 μm will not be completely volatilized in the total water instrument because of the short transit time needed for isokinetic flow. The background signal from the Lyman-α lamp at the detection axis is sensitive to particles and does in fact indicate that in some instances particles are incompletely vaporized. The background signal was used in conjunction with the particle size distributions to access when the TWI was producing accurate IWC measurements. Examination of this information indicated that possible incomplete vaporization resulted when the size distribution slope λ was less than about 150 cm^{-1}. Laboratory experiments are planned to quantify the scattering signal in the detection axis from water droplets as a function of diameter.

3. Results

[12] The effective densities of particle populations and for single particle sizes are characterized in this section using ice water content and particle size distribution data. Four WB-57F research flight days, 9, 11, 23, and 29 July, representing a total of 914 5-sec in-cloud data points are included in this study. Other days were omitted from this analysis either because of data quality issues or because the sampling was conducted in non-convectively generated cirrus. This section first looks at particle probe and total water instrument errors to identify the subset of the in-cloud periods that will yield reliable effective density values.

[13] *Brown and Francis* [1995] showed that the relationship

$$m(D)_{BF} = 0.00294 D^{1.9}, \quad (4)$$

the subscript referring to Brown and Francis, represented the $m(D)$ relationship for populations of mixed particle types observed in the ice clouds they sampled. In

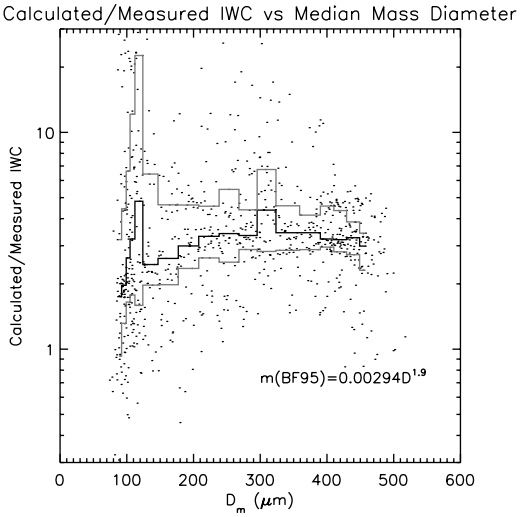

Figure 1. For 914 in cloud data points, the ratio of the IWC calculated using equation (4) to the measured IWC, plotted versus the median mass diameter of the size distribution. Median values are shown with the bold line and the 25th and 75th percentiles are shown with the thin lines.

equation (4) and hereafter, m is given in units of grams and D in cm. This relationship spanned a wide range of particle sizes, although there were few if any situations where the $m(D)_{BF}$ relationship could have been tested in exclusively sub-200 μm particle sizes. To test the Brown and Francis relationship in the generally colder (−55 to −73°C) and smaller particle-size situations sampled by the WB-57 during CRYSTAL-FACE, the product of the binned PSD and the particle mass (equation 4) was integrated over all size bins to obtain a "calculated" IWC_{BF} for each PSD. The median mass diameter, D_m, was derived from equation (3) and the fitted values of λ for each PSD. A value of $\varphi = 1.9$ is used in equation (3) from equation (4), although as noted earlier φ can range between about 1.7 to 3.0 for non-graupel ice particle types. Changing φ over this range leads to unimportant variations in D_m. Figure 1 shows the ratio IWC_{BF} to the measured IWC as a function of D_m. Beginning with a value of D_m of 50 μm where the TWI should completely vaporize particles, the IWC ratio increases progressively, then flattens at a ratio of about three. The Brown and Francis relationship apparently does not work reliably when particle sizes are small. The density implied by that relationship is always higher than the solid ice density of 0.91 g/cm^3 at sizes below 90 microns, and is forced to 0.91 g/cm^3 below that size. However, small ice crystals are not solid ice spheres but are non-spherical with a correspondingly lower effective density. Therefore, the Brown and Francis relationship tends to overestimate the IWC when applied to the small particle situations observed in this study. Nonetheless the results in Figure 1 may suggest the possibility that the measured IWC is underestimated where $D_m > 200$ μm. This is borne out by an examination of the TWI background signal data, which shows higher scattering values with decreasing values of D_m. We therefore take a conservative approach to minimize the potential for underestimation in $\overline{\rho_e}$ due to incomplete vaporization of particles in the TWI, and do not use any data where $D_m > 200$ μm, the net effect leading to a reduction in the number of acceptable 5-sec periods to 300.

[14] Of the accepted sample of data, errors in both the measured IWC and the population-total particle volume can lead to errors in the derived effective densities. If we assume that the concentration measurements are reliable and that we can estimate the maximum particle size to 20%, a reasonable estimate over all sizes, the total particle volume is accurate to about 54%. If we factor in the uncertainty in the IWC measurements of 10% for the periods that have been accepted on the basis of the values of λ, then a reasonable uncertainty of the population mean ensemble density values is ±56%. This value can be compared to the uncertainty from the application of the Brown and Francis relationship to the data of ± a factor of four, a significant improvement.

[15] A desirable outcome of this study would be the development of an effective density relationship that could be representative of the particle size distributions. Such a relationship could be used in modeling studies and remote sensing retrieval algorithms to derive the parameters described in Section 1 from a value of λ. For example, for a gamma distribution, particle volume is given by $\pi/6N_0\Gamma(4 + \mu)/\lambda^{4+\mu}$, and IWC = $\pi/6N_0\Gamma(4 + \mu)\overline{\rho_e}/\lambda^{4+\mu}$, and radar reflectivity is given by approximately $(\pi/6)^2(N_0)^2\Gamma(7 + \mu)/\lambda^{7+\mu}\overline{\rho_e}^2$, adjusting for appropriate units.

[16] Figure 2 shows the calculated particle ensemble mean densities ($\overline{\rho_e}$) as a function of λ for the entire dataset from the four WB-57F CRYSTAL cases. The dark boxes represent the data for $D_m < 200$ μm and the asterisks represent the median values sampled for λ intervals of 75 cm^{-1}, and the line is a least squares fit to the median values for $D_m < 200$ μm given by

$$\overline{\rho_e} = 0.00073\lambda^{1.125}. \quad (5)$$

[17] It is noted that for $D_m > 200$ μm (small dots in Figure 2) $\overline{\rho_e}$ continues to decrease with λ, although the extent of the decrease could be influenced by IWC underestimates. Results of Eq. 5 should be restricted to 0.91 g/m^3.

[18] Mass-dimension relations are important for converting size-dependent terms in particle size distributions (e.g.,

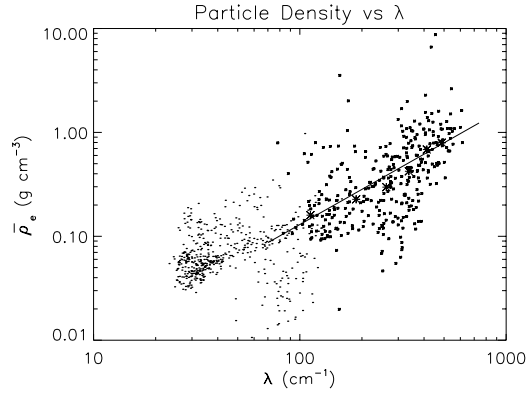

Figure 2. $\bar{\rho}_c$ versus λ for the entire dataset with the dark points showing $D_m < 200$ μm and the light points showing the remainder of the dataset. The asterisks represent the median values for 75 cm^{-1} intervals of λ. The solid line is a least squares fit to the median values.

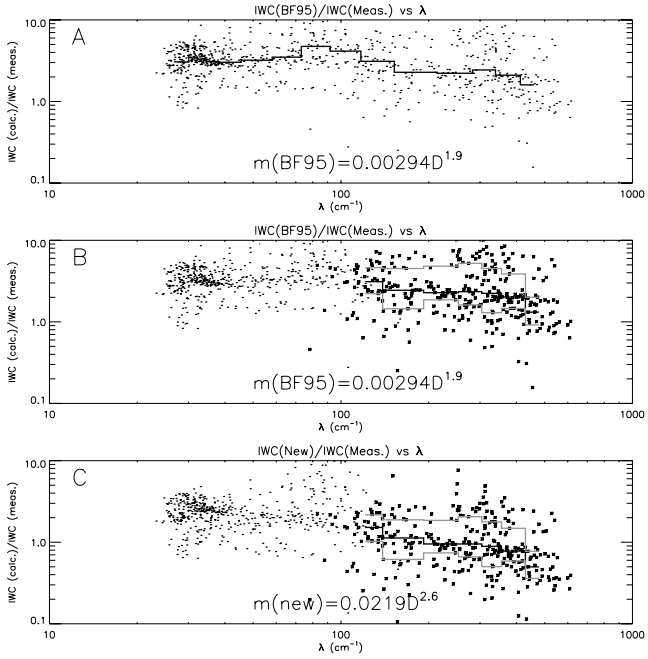

Figure 3. (a). The ratio of the IWC calculated using equation (4) to the measured IWC, plotted versus λ for the entire dataset. (b). Same as (a) except the points where D_m < 200 μm. (c). The ratio of ice water content calculated using equation (6) to the measured IWC, plotted versus λ. The median values are shown with the bold line and the 25th and 75th percentiles are shown with the thin lines on both plots.

terminal velocity) to bulk properties (e.g., precipitation rate). Figure 3a compares IWC_{BF} to the measured values. The Brown and Francis relationship appears on average to overestimate the observations.

[19] To find a refined $m(D)$ relationship, we vary the coefficient a and exponent b in the power-law relationship of the type used by Brown and Francis ($m = aD^b$) to find a "best" fit to the measured *IWC* across all λ. We focus on the portion of the dataset highlighted in Figure 3b where D_m < 200 μm. This corresponds to λ > 150 cm^{-1} in Figure 3a where there appears to be a discontinuity in the median values calculated from the Brown and Francis relationship. We derive the $m(D)$ relationship by using the measured (non-parameterized) size distributions and first varying b, between 1.7 to 2.7 in increments of 0.05, to find the *IWC*. This range represents the range of b values reported in the literature for various ice particle types. The a coefficient is first taken to the Brown and Francis value of 0.00294. The *IWC* calculated from this (a, b) pair are then compared to the measured values. The ratio, $\bar{r}$ = *IWC*(*calculated*)/*IWC*(*measured*) is averaged for all of the data points. A new a coefficient is then taken to be 0.00294/$\bar{r}$. The b value that produced the lowest value of the standard deviation of $\bar{r}$ yielded the best representation of the $m(D)$ relationship for all data points. The resulting relationship,

$$m(D) = 0.0219D^{2.6}, \tag{6}$$

produced the best fit to the data for D_m < 200 μm. D is in centimeters and m is in grams. This equation gives a density of 0.91 or less for particles larger than 4.5 μm. Figure 3c shows the results using the relationship developed with the technique described above. Overall, this new relationship produces very good results over a wide range of λ. Note that this relationship overestimates the IWC values for D_m > 200 μm, which were not included in the curve fit.

[20] Analytic representations for the *IWC* can now be obtained in terms of the PSD fit parameters and the population-mean density or the mass-dimensional relationships developed earlier in this section. The equation for particle volume (equation 1) and the PSD functional form (equation 2) can be integrated over all sizes from 0 to ∞ (a very good approximation with little error because of typical values of λ) to yield

$$IWC = \overline{\rho_e}V = (\pi/6)\overline{\rho_e}\int_0^\infty N_0 e^{-\lambda D} D^{(3+\mu)} dD = 0.00073 \lambda^{1.125}\left[(\pi/6)N_o\Gamma(4+\mu)/\lambda^{(4+\mu)}\right]. \tag{7}$$

where particle volume is from equation (5) and is not part of the integration. Alternatively, equation (6) can be used to specify particle mass in terms of particle dimension and is part of the integration, yielding

$$IWC = \int_0^\infty m(D)N(D)dD = 0.0219N_0\Gamma(3.6+\mu)/\lambda^{(3.6+\mu)}. \tag{8}$$

equations (7) and (8) apply to cold anvil cirrus and do not apply to situations where particles are predominantly large and λ values are low.

4. Summary and Conclusions

[21] This study uses measured condensed water contents and particle size spectrometer measurements in cold cirrus anvils during CRYSTAL FACE to derive the mean effective ice particle densities for ice particle populations, and as a function of size within the population. This study extends earlier observations of ice particle densities and masses that have been obtained primarily at the ground or in cloud for populations containing large particles at warmer temperatures. It has the added benefit of measurements made directly in the tops of anvils that are crucial for radiative transfer studies. We have limited our analysis for PSD where the median mass diameters are smaller than 200 μm or λ > 150 cm^{-1}, where we are confident of our results. The method can be extended to larger values of D_m, with further laboratory evaluation of the IWC measurements when large particles are present that suggest a different $m(D)$ relationship than given by equation (6).

[22] Analytic expressions are developed to derive the *IWC*, either from size distribution measurements from aircraft (from which the total volume of the particle population per unit volume of air is derived) or from coefficients for gamma or exponential fits to the PSD. The fit coefficients λ and μ can be estimated from the air temperature [*Ryan*, 2000; *Heymsfield et al.*, 2002], and N_o can be estimated from radar data or some knowledge of the *IWC* itself. The expressions developed here can be used to improve estimates of *IWC* from past data sets where direct measurements of *IWC* were unavailable.

[23] **Acknowledgments.** The NASA CRYSTAL program through NASA-NSF agreement number W-10, 024, and NASA grants NAG5-11548 and NAG-511547 supported this research, Don Anderson program manager. The authors are indebted to the crew of the WB57-F aircraft for their outstanding efforts with the data collection.

References

Baumgardner, D., G. Raga, G. Kok, B. Anderson, A. Heymsfield, P. Lawson, B. Baker, A. Strawa, T. Garrett, E. Weinstock, and J. Smith (2004), Morphology of Tropical Cirrus Crystals Derived from Single Particle and Bulk Property Analysis, *J. Geophys. Res.*, in press.

Brown, P. R. A., and P. N. Francis (1995), Improved measurements of the ice water content in cirrus using a total-water probe, *J. Atmos. Oceanic Technol.*, *12*, 410–414.

Heymsfield, A. J. (1972), Ice crystal terminal velocities, *J. Atmos. Sci.*, *29*, 1348–1357.

Heymsfield, A. J., and J. L. Parrish (1978), A computational technique for increasing the effective sampling volume of the PMS 2-D particle size spectrometer, *J. Appl. Meteorol.*, *17*, 1566–1572.

Heymsfield, A. J., A. Bansemer, P. R. Field, S. L. Durden, J. Stith, J. E. Dye, W. Hall, and T. Grainger (2002), Observations and parameterizations of particle size distributions in deep tropical cirrus and stratiform precipitating clouds: Results from in-situ observations in TRMM field campaigns, *J. Atmos. Sci.*, *59*, 3457–3491.

Heymsfield, A. J., A. Bansemer, C. Schmitt, C. Twohy, and M. R. Poellot (2004), Effective ice densities from aircraft data, *J. Atmos. Sci.*, in press.

Locatelli, J. D., and P. V. Hobbs (1974), Fall speeds and masses of solid precipitation particles, *J. Geophys. Res.*, *79*, 2185–2197.

Magono, C., and T. Nakamura (1965), Aerodynamic studies of falling snowflakes, *J. Meteorol. Soc. Japan*, *43*, 139–147.

Mitchell, D. L. (1991), Evolution of snow-size spectra in cyclonic storms. Part II: Deviations from the exponential form, *J. Atmos. Sci.*, *48*, 1885–1899.

Ryan, B. F. (2000), A bulk parameterization of the ice particle size distribution and the optical properties in ice clouds, *J. Atmos. Sci.*, *51*, 1436–1451.

Weinstock, E. M., et al. (1994), New fast response photofragment fluorescence hygrometer for use on the NASA ER-2 and the Perseus remotely piloted aircraft, *Rev. Sci. Instrum.*, *65*, 3544–3554.

Weinstock, E. M., et al. (2003), Total water measurements on the WB57 aircraft in thin and thick cirrus, *J. Geophys. Res.*, (in preparation).

A. Bansemer, A. J. Heymsfield, and C. G. Schmitt, National Center for Atmospheric Research, Boulder, CO 80301, USA. (schmittc@ucar.edu)

D. Baumgardner, Universidad Nacional Autonoma de Mexico, 04510 Mexico City, Mexico.

D. Sayres, J. T. Smith, and E. M. Weinstock, Harvard University, Cambridge, MA, USA.